Nature of the Transition Structure for Alkene Epoxidation by Peroxyformic Acid, Dioxirane, and Dimethyldioxirane: A Comparison of B3LYP Density Functional Theory with Higher Computational Levels

Robert D. Bach,*[1a] Mikhail N. Glukhovtsev,[1a] Carlos Gonzalez,[1b] Manuel Marquez,[1d] Carlos M. Estévez,[1a] Anwar G. Baboul,[1c] and H. Bernhard Schlegel[1c]

Department of Chemistry and Biochemistry, University of Delaware, Newark, Delaware 19716, Pittsburgh Supercomputing Center, Carnegie Mellon University, Pittsburgh, Pennsylvania 15213, Department of Chemistry, Wayne State University, Detroit, Michigan 48202, and Department of Chemistry, Yale University, New Haven, Connecticut 06520

Received: January 30, 1997[⊗]

The performance of the B3LYP density functional theory calculations has been studied for the epoxidation reactions of ethylene, propene, and *cis*- and *trans*-2-butene with peroxyformic acid and of ethylene with dioxirane and dimethyldioxirane. The transition structures for the epoxidation of ethylene and propene with peroxyformic acid and of ethylene with dioxirane and dimethyldioxirane calculated at the B3LYP level as well as at the QCISD and CCSD levels are symmetrical with nearly identical C−O bond distances, whereas the MP2 calculations favor unsymmetrical transition structures. The geometrical parameters of the transition structures calculated using the B3LYP functional are close to those found at the QCISD and CCSD levels. While the activation barriers for the epoxidation reactions calculated at the B3LYP/6-31G* and B3LYP/6-31+G* levels are very close to the MP4SDTQ/6-31G*//MP2/6-31G* and MP2/6-31G*//MP2/6-31G* values, these activation energies are systematically lower (up to 5−6 kcal/mol) than the barrier heights calculated at such higher correlated levels as the QCISD(T)/6-31G*//QCISD/6-31G*, CCSD(T)/6-31G*//CCSD/6-31G*, and BD(T)/6-31G*//QCISD/6-31G*. The calculations on the epoxidation reactions of ethylene and propene with peroxyformic acid using the BH&HLYP functional also lead to symmetrical transition structures, but the calculated barriers are overestimated when compared with the QCISD(T) results. The activation barriers calculated for these epoxidation reactions at the QCISD(T)/6-31G*//B3LYP/6-31G* level are very close to those computed at the QCISD(T)/6-31G*//QCISD/6-31G* level.

1. Introduction

Recent years have witnessed the growing popularity of density functional theory (DFT)[2a,b] methods as computationally low-cost approximations for treating electron correlation in inorganic, organic, and organometallic molecules.[2] These methods employ both "gradient-corrected"[3] and hybrid approaches[4] in which the Hartree−Fock "exact exchange" is also included in the functional. Among various proposed functionals, the Becke's three-parameter hybrid functional[3a,4a] combined with the Lee, Yang, and Parr (LYP) correlation functional,[3b] denoted as B3LYP,[4b] appears to be the functional form which yields good results in calculations of molecular structure and energetics.[2g−i,k,5−7] Some recent studies have evaluated the performance of the B3LYP calculations of reaction profiles.[7] The B3LYP calculations of the prototype ion−molecule gas-phase S_N2 reactions, $CH_3Cl + Cl^-$ and $CH_3Br + Cl^-$, have shown[7a] that the central barrier heights (8.7 and 5.0 kcal/mol) are underestimated at the B3LYP/6-311+G(3df,2p)//B3LYP/6-31+G(d) level as compared with the G2(+) computational results (13.3 and 9.4 kcal/mol) and the experimental data (13.2 ± 2 and 10.7 kcal/mol). The comparison of the B3LYP/6-31G* calculated activation barriers for the $H_2SO \rightarrow HSOH$, $F_2SS \rightarrow FSSF$, and $HNC \rightarrow HCN$ gas-phase rearrangements with that computed at the QCISD/6-31G* level revealed that the B3LYP calculated barriers were also systematically underestimated.[7b] An underestimated barrier value for the $F + H_2 \rightarrow HF + H$ radical reaction was found[7c] by the B3LYP/6-311++G(3df,3pd) calculations (0.07 kcal/mol) as compared with the calculated QCISD(T)/6-311++G(3df,3pd) barrier (1.86 kcal/mol) and the experimental value (2.0 kcal/mol). The B3LYP/6-311G(d,p) calculations lead to a barrier of 8.03 kcal/mol for the $H + N_2 \rightarrow HN_2$ reaction, whereas the CASSCF/CCI calculations give a value of 15.20 kcal/mol.[7d]

For some reactions the B3LYP calculated barriers are in good agreement with the experimental data and the results of higher level calculations. For example, for the $H + N_2O \rightarrow HON_2$ reaction, which is similar to the $H + N_2 \rightarrow HN_2$ reaction discussed above, the B3LYP/6-311G(d,p) calculated barrier (13.91 kcal/mol) is close to that (14.60 kcal/mol) calculated at the G2 level.[7d] The calculated B3LYP/6-311+G(d,p) barrier (53.0 kcal/mol) for the $HOOH \rightarrow OOH_2$ rearrangement also agrees well with the CCSD(T)/TZ2P+f value of 54.8 kcal/mol.[7e] B3LYP predicted barrier heights for the concerted pathway for the Diels−Alder reaction of 1,3-butadiene and ethylene were found to be in excellent agreement with the experimental data.[7f] The barrier heights of the gas-phase reactions of halobenzenes with halide anions, calculated at the B3LYP/6-31+G(d) level, are very close to the MP2/6-31+G(d) values.[7g] Therefore, the computational results reported in the literature to date do not allow any definitive conclusion about the performance of the B3LYP functional in calculations of reaction barriers. It is likely that this overall performance varies considerably depending upon the reaction type.

The present study addresses the performance of the DFT methods for calculations of alkene epoxidation reactions which exemplify an important type of oxygen transfer process.[8] Our previous results have shown that reaction profiles of those reactions involving the O−O bond are very sensitive to the level of theory.[9] We found that electron correlation contributions,

⊗ Abstract published in *Advance ACS Abstracts,* August 1, 1997.

S1089-5639(97)00378-2 CCC: $14.00

at least at the MP2 level, were essential to getting reliable thermochemical data for O−O bond cleavage.[10] The transition structures may also exhibit multireference character and require treatments that take into account nondynamical correlation. Therefore, these alkene epoxidation reactions represent a challenge for computational chemistry. In the present study the results of high-level calculations on the epoxidation reactions are discussed in order to provide a comparison with the DFT data, affording an excellent opportunity to evaluate the performance of such new computational methods as DFT theory. Can density functional methods based on nonlocal functionals be capable[11] of providing a reliable description of these reactions where nondynamic near-degeneracy correlations may be important in addition to dynamical many-particle correlations? If the application of this method proves to be successful, it will open a way to explore computationally the mechanisms of epoxidation of larger alkenes and the effects of various substituents on the epoxidation rates—a topic whose history can be traced back for at least a half-century.[12]

2. Computational Methods

Ab initio molecular orbital calculations[13] were performed with the GAUSSIAN 94 system of programs.[14] The Becke three-parameter hybrid functional[3a,4a] combined with Lee, Yang, and Parr (LYP) correlation functional,[3b] denoted B3LYP,[4b] was employed in the calculations using density functional theory (DFT):

$$E_{xc}^{B3LYP} = (1 - a_o)E_x^{LSDA} + a_o E_x^{HF} + a_{x\Delta}E^{B88} + a_c E_c^{LYP} + (1 - a_c)E_c^{VWN} \quad (1)$$

$$(a_o = 0.20;\ a_x = 0.72;\ a_c = 0.81)$$

In eq 1 E_x^{HF} is the Hartree−Fock exchange, E_x^{LSDA} denotes the local (Slater) exchange energy from local spin density approximation (LSDA), ΔE^{B88} is Becke's gradient correction to the exchange functional,[3a] E_c^{LYP} is the correlation functional developed by Lee, Yang, and Parr,[3b] and E_c^{VWN} is the correlation energy calculated using the local correlation functional of Vosko, Wilk, and Nissair (VWN). Geometries were optimized[15] at the B3LYP, MP2, QCISD,[16] and CCSD[17] levels using either the 6-31G* or the 6-31+G* basis sets.[13] The energies were refined by single-point calculations at the MP4SDTQ, QCISD(T),[16] CCSD(T),[17] BD, and BD(T) (Brueckner doubles including a perturbation correction for triple excitations (BD(T))[18] levels of theory. The stationary points on the potential energy surfaces were characterized by calculations of vibrational frequencies.[13,15] Zero-point energies (ZPE) computed at the B3LYP/6-31G* and B3LYP/6-31+G* levels were scaled by 0.98 according to Bauschlicher and Partridge.[5c] The geometry of the transition structure for ethylene epoxidation by peroxyformic acid was optimized at the CCSD(T) and CASSCF[19] levels as well (using the ACES program).[20] We have also carried calculations on the epoxidation of ethylene and propene with peroxyformic acid using the BH&HLYP functional.[21,22] Throughout the text, bond lengths are in angstroms and bond angles are in degrees.

3. Results and Discussion

Epoxidation of Ethylene by Peroxyformic Acid. The mechanism for alkene epoxidation by peroxyacids that has been generally accepted was initially proposed by Bartlett[12] 46 years ago. He suggested a mechanism involving a cyclic polar process in which the proton of the peroxyacid is received by the carbonyl oxygen simultaneously with attack on the alkene double bond (eq 2):

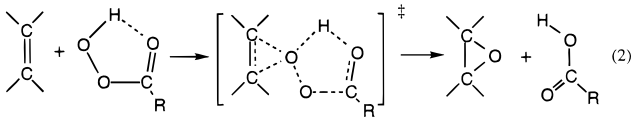

Supporting evidence for this mechanism has been provided by a number of research groups,[23] and as a result of the overall shape of this planar transition structure the term "butterfly mechanism" came into general use. We suggested[9a,b] that a spiro orientation, where the plane of the peroxyacid functional group is at right angles to the axis of the carbon−carbon double bond, would be lower in energy if the oxygen lone pair of electrons interacted strongly with the π^* orbital or the alkene π bond. The electrophilic character of the peroxo functionality is ascribed to the fact that it has a relatively weak O−O σ bond that when experiencing bond elongation upon attack by a nucleophile induces its empty σ^* O−O orbital to accept electron density.[9b]

(a) MP2 Calculations. In our previous studies we have found two types of transition structures for the epoxidation of ethylene by peroxyformic acid.[9c,f] We reported a symmetrical spiro-orientated transition structure initially, where the two developing C−O bonds were of equal length[9c] (however, it is a second-order saddle point at the MP2/6-31G* level), that lies ∼0.2 kcal/mol higher in energy (at the MP4SDTQ/6-31G*//MP2/6-31G* level) than the unsymmetrical first-order saddle point (**1a**). This small energy difference shows that this potential energy surface is rather flat. We also reported a highly unsymmetrical transition structure at the MP2 level with the C−O bond lengths of 1.805 and 2.263 Å but pointed out that higher correlated levels of theory suggested a symmetrical transition structure.[9f,24] We also addressed the question of symmetrical vs unsymmetrical approaches of the electrophilic oxygen within the context of the behavior of various nucleophiles toward peroxyformic acid. The restricted Hartree−Fock solution for the symmetrical "transition structure" optimized with symmetry constraints (at the MP2/6-31G* geometry) exhbits a triplet (restricted Hartree−Fock (RHF) → (UHF) unrestricted Hartree−Fock) instability.[26] Hence, in order to resolve the question of a symmetrical vs an unsymmetrical approach of the electrophilic oxygen to the carbon−carbon double bond, a study of reaction 2 (R = H) at higher correlated levels is necessary and we have to consider the results of higher level conventional ab initio calculations before discussing data of the B3LYP calculations.

(b) QCISD, CCSD, QCISD(T), and CCSD(T) Calculations. Full geometry optimization at the QCISD/6-31G* level afforded a symmetrical spiro transition structure **1b** (Table 1, Figure 1) in which the dihedral angle between the planes of the two reactants is approximately 91° and the carbon−oxygen bond distances are both 2.006 Å, in contrast to the MP2 calculations that lead to an unsymmetrical structure (Figure 1). The activation barriers for the fully optimized MP2 and QCISD transition structures calculated at the QCISD(T) level are 19.9 and 18.8 kcal/mol, respectively. The $\Delta E^{\ddagger}$ at the QCISD(T)/6-31G*//QCISD/6-31G* level is 2.5 kcal/mol higher in energy than the corresponding MP4//MP2/6-31G* barrier height. As anticipated, geometry optimization at the CCSD/6-31G* level also led to a symmetrical transition structure very close to that obtained at QCISD. Since the triple excitations markedly influence the activation barrier for ethylene epoxidation, we thought it essential to examine their effect upon the geometry. Using analytical gradients for CCSD(T) wave functions[18] we reoptimized the CCSD geometry of the transition structure and

TABLE 1: Geometrical Parameters of the Transition Structure for the Epoxidation of Ethylene Calculated at Various Levels of Theory[a,b]

	MP2/6-31+G* (MP2/6-31G*) **1a**	QCISD/6-31G* **1b**	CCSD(T)/6-31G* (CCSD/6-31G*) **1b**	CASSCF(10,10)/6-31G* **1b**	B3LYP/6-31+G* (B3LYP/6-31G*) **1b**	BH&HLYP/6-31G* **1b**
O_2-O_1	1.765 (1.768)	1.866	1.893 (1.860)	1.893 (1.876)[c]	1.857 (1.855)	1.843
O_1-C_1	1.827 (1.805)	2.006	1.977 (1.976)	2.019 (2.049)	2.043 (2.026)	1.922
O_1-C_2	2.292 (2.263)	2.006	1.977 (1.974)	2.019 (2.049)	2.051 (2.031)	1.922
O_2-C_3	1.329 (1.319)	1.296	1.296 (1.288)	1.285 (1.277)	1.290 (1.289)	1.267
O_3-C_3	1.228 (1.230)	1.242	1.246 (1.242)	1.217 (1.216)	1.239 (1.239)	1.230
O_3-H_1	1.843 (1.830)	1.681	1.666 (1.653)	1.772 (1.745)	1.727 (1.687)	1.618
O_1-H_1	0.998 (0.997)	1.010	1.014 (1.012)	0.970 (0.972)	1.006 (1.010)	1.002
$\angle O_2-O_1-C_1$	153.5 (152.6)	159.6	159.2 (159.4)	159.9 (160.2)	160.2 (160.0)	159.7
$\angle O_2-O_1-C_2$	169.0 (169.2)	159.6	159.0 (159.2)	160.0 (160.3)	160.6 (160.2)	159.7
$\angle O_1-C_1-C_2$	90.1 (89.5)	70.0	69.6 (69.6)	70.2 (70.5)	70.1 (70.1)	70.1
$\angle H_1-O_1-O_2$	92.1 (91.3)	82.7	81.7 (82.0)	83.3 (83.9)	84.0 (83.1)	81.4
$\angle O_1-O_2-C_3$	103.8 (103.9)	102.4	101.6 (102.3)	103.6 (103.3)	103.6 (102.8)	102.5
$\angle O_2-C_3-O_3$	127.1 (127.3)	125.8	126.1 (125.5)	126.0 (125.9)	125.8 (126.0)	125.0
$\angle C_3-O_3-H_1$	86.4 (85.8)	86.8	86.9 (86.8)	87.3 (87.6)	86.9 (86.7)	87.1
$\angle C_3-O_2-O_1-H_1$	4.1 (4.4)	0.0	0.4 (0.1)	0.0 (0.0)	0.1 (0.1)	0.0
$\angle H_1-O_1-C_1-C_2$	54.1 (59.4)	91.1	91.4 (91.4)	91.2 (91.0)	92.1 (91.2)	91.5

[a] Bond distances are in angstroms; bond angles are in degrees. [b] The numbering of the atoms in unsymmetrical (**1a**) and symmetrical (**1b**) transition structures are shown in Figure 1. [c] The CASSCF(10,9) values are given in parentheses.

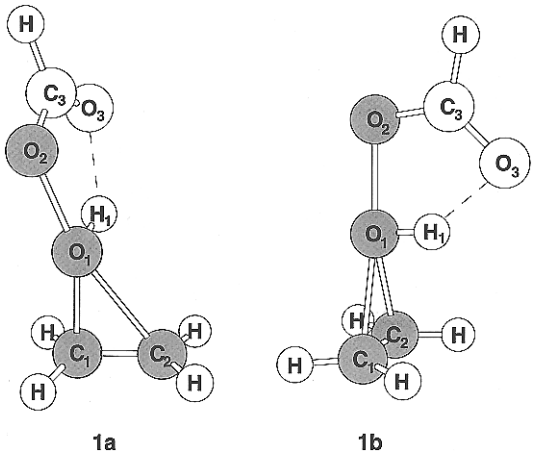

Figure 1. The unsymmetrical (**1a**) and symmetrical (**1b**) transition structures for the epoxidation of ethylene with peroxyformic acid. Their geometrical parameters are listed in Table 1.

found very comparable results to those obtained in the absence of the triples (Table 1).

(c) BD Calculations. We also investigated the use of the Brueckner doubles (BD) model. The BD wave function is closely related to the QCISD and CCSD wave functions but differs in that the contribution of single excitations is eliminated by explicit transformation of the orbitals. Hence, in the BD model the orbitals relax in the presence of the dynamic correlation (double excitations). We carried out BD and BD(T) calculations on the MP2 and QCISD geometries. The barriers alter slightly at the BD(T)/6-31G* level to 20.3 and 19.9 kcal/mol (Table 2), but the trend remains the same indicating that the QCISD and CCSD treatment of the orbital correction is adequate. Therefore, on the basis of our previous experience and the nature of the four wave functions we have used, we believe that the QCI and CC methods are probably the most reliable for this system. Despite the significant discrepancy in geometry, the QCISD(T)//QCISD and MP4//MP2 barriers are very similar for both geometries. The BD(T)/6-31G*//MP2/6-31G* (**1a**) and BD(T)/6-31G*//QCISD/6-31G* (**1b**) energy difference between the activation barriers for unsymmetrical (**1a**) and symmetrical (**1b**) transition structures, respectively, also remains very small (0.4 kcal/mol, Table 2). This suggests that the back-bonding between the oxygen lone pair and the π^* orbital of ethylene in the spiro orientation is also small but is sufficient to insure a spiro geometry.[9a,b]

TABLE 2: Activation Barriers (in kcal/mol) for the Epoxidation of Ethylene with Peroxyformic Acid Calculated at Various Computational Levels[a]

computational level	$\Delta E^{\ddagger}$
(Unsymmetrical TS, **1a**)	
MP2/6-31G*//MP2/6-31G*	16.5
MP2/6-31G**//MP2/6-31G**	16.9
MP2/6-31+G*//MP2/6-31+G*	14.0
MP2/6-311+G*//MP2/6-311+G*	15.5
BD/6-31G*//MP2/6-31G*	29.1
MP4SDTQ/6-31G*//MP2/6-31G*	16.3
QCISD(T)/6-31G*//MP2/6-31G*	19.9
BD(T)/6-31G*//MP2/6-31G*	20.3
(Symmetrical TS, **1b**)	
QCISD/6-31G*//QCISD/6-31G*	25.1
BD/6-31G*//QCISD/6-31G*	28.5
QCISD(T)/6-31G*//QCISD/6-31G*	18.8
BD(T)/6-31G*//QCISD/6-31G*	19.9
CCSD/6-31G*//CCSD/6-31G*	27.3
CCSD(T)/6-31G*//CCSD/6-31G*	19.4
B3LYP/6-31G*//B3LYP/6-31G*	14.1 (14.7)[b]
B3LYP/6-31+G*//B3LYP/6-31+G*	15.2 (16.3)[b]
QCISD(T)/6-31G*//B3LYP/6-31G*	18.7
BH&HLYP/6-31G*//BH&HLYP/6-31G*	26.9 (27.5)[b]

[a] Barrier heights are relative to the isolated reactants. [b] The barrier values including zero point corrections (the ZPE values were scaled with 0.98) are shown in parentheses.

(d) CASSCF Calculations. Nondynamical correlation may also have an important influence on this reaction and can be assessed by CASSCF computations. The choice of active spaces is a crucial question in carrying out CASSCF calculations.[19] Reliable geometries can also be obtained by CASSCF calculations provided a sufficient virtual space is included to adequately describe the delocalization of negative charge in the developing formate anion in both its σ and π virtual space. Initially the orbitals were chosen by inspection of the unrestricted Hartree−Fock natural orbitals (UNO)[27] at transition state geometries **1a** and **1b** obtained at the MP2 and QCI levels, respectively. At both geometries the UNO suggested that only four electrons and four orbitals should be active. When the active space included only two virtual orbitals (4, 4), the peroxy moiety moved in large steps along the double bond until an unsymmetrical structure resembling that at MP2 was obtained.[28]

The active space was systematically extended to include all occupied orbitals with orbital coefficients on the ethylene fragment and also three oxygen lone pair orbitals (one from each oxygen atom). The virtual space was also extended by one orbital, corresponding to the O−C−O fragment π orbital. This space now consisted of 14 electrons in 10 orbitals (14, 10). The geometry was reoptimized but still remained as a highly unsymmetrical structure. Relative to the (4, 4) geometry, the O−O distance is reduced from 2.079 to 1.992 Å, while the incipient C−O bond is reduced from 1.864 to 1.817 Å. In comparison with the MP2 geometry, the CASSCF produces an excessively long peroxy O−O bond (1.992 Å vs 1.768 Å) and a slightly more extended incipient C−O bond (1.817 Å vs 1.805 Å). In addition, the MP2, QCISD, and CCSD structures show a short hydrogen bond distance of 1.830, 1.681, and 1.65 Å, respectively, between the peroxy hydrogen and the carbonyl oxygen. In the CASSCF structure this distance is lengthened to 2.070 Å. The natural orbital occupancies of the 14 electron/10 orbital calculation are 1.99, 1.99, 1.99, 1.99, 1.95, 1.92, 1.57, 0.45, 0.08, and 0.06. When the barrier is recalculated at the MP2 level using the CASSCF (14, 10) structure, these factors contrive to give a destabilization of 10.8 kcal mol^{-1} which led us to question the active space chosen.

We looked next at a single-point CASSCF (14, 10) calculation using the symmetric QCISD geometry. The depopulation of the HOMO is much reduced (occupancy = 1.85) relative to the unsymmetrical MP2 structure. The orbitals are superpositions of the bonding and antibonding O−O orbitals and the ethylene π and π^* orbitals.

A thorough CASSCF analysis of the problems associated with symmetry breaking in the formyloxy radical ($HCO_2^{\bullet}$) emphasized the necessity for inclusion of virtual orbitals corresponding to both the σ and π O−C−O fragment orbital.[29] When this σ O−C−O virtual orbital was added to the active space and the two lowest occupied orbitals (both with orbital occupations >1.99) were removed, the active space consisted of 10 electrons in nine orbitals. Geometry optimization at this level, (10, 9) afforded a symmetrical transition structure that is remarkably close to that obtained at the QCISD level (Table 1). The importance of the additional virtual orbital is further implicated when one notes the fact that the number of excitations in the (14, 10) and (10, 9) calculations are not that different.[30] When an additional σ O−C−O fragment virtual orbital was added (10, 10), very little change in geometry was observed. The natural orbital occupancies of the 10 electron, 10 orbital active space with 19 404 excitations are 1.98, 1.96, 1.92, 1.95, 1.90, 0.15, 0.06, 0.06, 0.01, and 0.01. Significantly, the electron occupation of virtual orbitals in this (10, 10) calculation is 0.3 electrons less than that predicted by the above (14, 10) calculation. The relative depopulation of the σ^* O−O orbital by including the additional σ and π O−C−O virtual orbitals in the active space resulted in a shortened (0.10 Å) O−O bond distance and a distinctively different transition state geometry. A single-point QCISD(T) calculation on this (10, 10) geometry differed by only 1.82 kcal/mol from the fully optimized QCISD transition state.

(e) Comparison of the MP2, QCI, CC, BD, and CASSCF Computational Results. The MP2 and CASSCF geometries for ethylene epoxidation with limited virtual space (14, 10) are both unsymmetrical while the QCISD, CCSD, CCSD(T), and the (10, 9) and (10, 10) CASSCF calculations give symmetrical transition structures. In this series of papers[9] we have contended that in the description of oxygen transfer reactions the dynamical electron correlation is more critical than the static or nondynamical correlation effects. The CASSCF model is designed for recovering the effects of static correlation, while the MP2 method provides a low-order description of dynamical correlation. The QCI and CC methods recover higher order correlation effects by taking certain terms in the perturbation expansion to infinite order. In addition, since the single excitations are included, the QCISD and CCSD have an implicit orbital correction term, although this is only reflected in the QCI and CC weights rather than explicitly in the orbitals. Therefore, we conclude that the ethylene epoxidation with peroxyformic acid proceeds via a symmetrical spiro transition structure. A similar situation has been found for the acid-catalyzed epoxidation of ethylene.[9g]

(f) DFT (B3LYP) Calculations. The B3LYP/6-31G* and B3LYP/6-31+G* calculations carried out without any restrictions of symmetry resulted in an almost symmetrical transition structure **1b** (Table 1; Figure 1), in contrast to the MP2 calculations but in agreement with the QCISD, CCSD, CCSD(T), BD(T), and CASSCF (10, 9) calculations discussed above. It is notable that whereas the RHF solution at the B3LYP-optimized symmetrical transition structure is triplet unstable, the B3LYP solution is stable. The difference between the two developing O−C bond lengths in the transition structure calculated using B3LYP/6-31+G* is only 0.008 Å, in contrast to the difference of 0.465 Å at the MP2/6-31+G* level (Table 1). The predicted B3LYP/6-31G* and B3LYP/6-31+G* barriers are 14.1 and 15.2 kcal/mol, respectively. These barriers, however, are lower than those found at the QCISD(T)/6-31G*//QCISD/6-31G* and CCSD(T)/6-31G*//CCSD/6-31G* levels (19.4 and 18.8 kcal/mol, respectively) (Table 2). These B3LYP barrier heights differ just slightly from the MP2 and MP4SDTQ values (Table 2).

The transition structure geometries obtained at the B3LYP level, however, are remarkably close to those optimized at such more time-consuming levels of theory as CCSD, CCSD(T), and QCISD (Table 1). The QCISD(T)/6-31G* barrier calculated using the B3LYP/6-31G* optimized geometries (18.7 kcal/mol) is very close to that found at the QCISD(T)/6-31G*//QCISD/6-31G* level (Table 2). This procedure (QCISD(T)//B3LYP/6-31G* can be apparently used as a computer-time economical protocol for such electronically impaired transition structures as those for alkene epoxidation.

Epoxidation of Propene with Peroxyformic Acid. For an alkyl-substituted alkene such as propene, conventional wisdom suggests that an electrophilic reagent should attack the least substituted carbon atom in a Markovnikov fashion. However, at the MP2/6-31G* level the activation barrier for approaching the more substituted carbon atom (**2a**, Figure 2) is actually 0.2 kcal/mol lower in energy than attack at the terminal methylene group (**2b**, Table 3). Surprisingly, both of these structures are first-order saddle points at the MP2/6-31G* level. We have also examined the epoxidation of propene at the QCISD/6-31G* level, and as anticipated based upon results with ethylene, a single more central nearly spiro transition structure **2c** ($\angle C_3O_2C_1C_2 = 89.8°$) for attack of the carbon−carbon double bond is found. The bond distances between the spiro oxygen and the double-bond carbons are 2.016 and 2.037 Å, just slightly favoring the Markovnikov orientation at the QCISD/6-31G* level. These C−O bond distances are 2.005 and 2.122 Å at the B3LYP/6-31G* level, whereas the distances are 1.821 and 2.248 Å (**2a**) at the MP2/6-31G* level, Figure 2). The calculations at the B3LYP/6-31G* level also lead to a more central transition structure but with a lower barrier (12.4 kcal/mol, Table 3, $\angle C_3O_2C_1C_2 = 93.7°$). Interestingly, an $E_a^{\ddagger}$ value of 11.8 kcal/mol has been reported for propylene oxide formation by the action of peroxyacetic acid in benzene

TABLE 3: Activation Barriers (in kcal/mol) for the Epoxidation of Propene with Peroxyformic Acid Calculated at Various Computational Levels[a]

	$\Delta E^{\ddagger}$					
substrate	MP2/6-31G*// MP2/6-31G*	MP4SDTQ/6-31G*// MP2/6-31G*	QCISD(T)/6-31G*// QCISD/6-31G*	B3LYP/6-31G*	QCISD(T)/6-31G*// B3LYP/6-31G*	BH&HLYP/6-31G*
ethylene	16.5	16.3	18.8 (25.1)[c]	14.1[d]	18.7 (16.0)[f]	26.9
propene	13.8[b]		16.0 (22.3)[c]	12.0[d,e]	15.9 (12.8)[f]	24.5[g]

[a] The barrier heights are relative to the reactants. The barriers for the ethylene epoxidation are given for the sake of comparison. [b] The MP2/6-31G* barrier is given for transition structure **2b**. The MP2/6-31G* and MP4SDTQ/6-31G*//MP2/6-31G* barriers for transition structure **2a** are 13.6 and 11.2 kcal/mol, respectively. [c] The QCISD/6-31G*//QCISD/6-31G* values are shown in parentheses. [d] 14.6 kcal/mol at the B3LYP/6-31+G* level. [e] 12.3 kcal/mol with the ZPE(B3LYP/6-31G*) correction. The ZPE values were scaled with 0.98. The transition structure **2d** is 0.4 kcal/mol higher in energy than **2c**. [f] The MP4SDTQ/6-31G*//B3LYP/6-31G* values are given in parentheses. [g] 24.7 kcal/mol with the ZPE(BH&HLYP/6-31G*) correction. The ZPE values were scaled with 0.98.

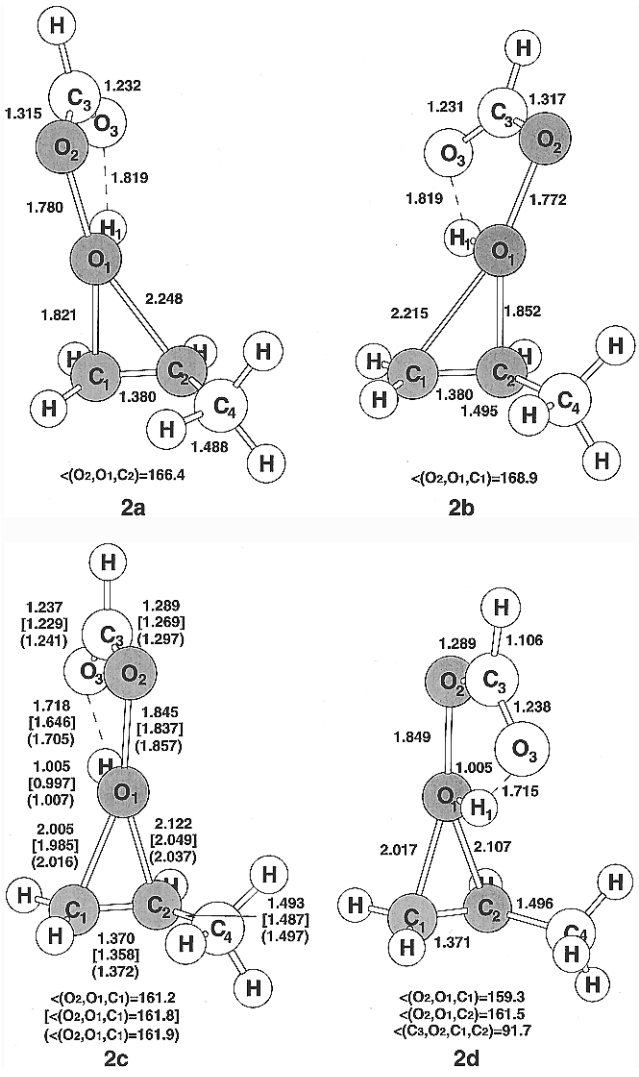

Figure 2. Selected geometrical parameters of the transition structures for the epoxidation of propene with peroxyformic acid calculated at the MP2/6-31G* (**2a** and **2b**), the B3LYP/6-31G* (**2c**), and QCISD/6-31G* levels (**2c**). For structure **2c**, the geometrical parameters calculated at the QCISD/6-31G* and BH&HLYP levels are given in parentheses and square brackets, respectively. The transition structure (**2d**) with "endo" orientation of the HOOCO fragment is higher in energy than **2c** (Table 3).

solvent.[31] The QCISD/6-31G*//QCISD/6-31G* and QCISD(T)//QCISD/6-31G* classical ($\Delta E^{\ddagger}$) barriers for the epoxidation of propene are somewhat higher and are predicted to be 22.3 and 16.0 kcal/mol, respectively. The effect of the triples contributions in significantly lowering the barrier height is again noted for propene. The QCISD(T)/6-31G*//B3LYP/6-31G* barrier height (15.9 kcal/mol) is remarkably close to the QCISD(T)//QCISD/6-31G* value (16.0 kcal/mol) (Table 3). The

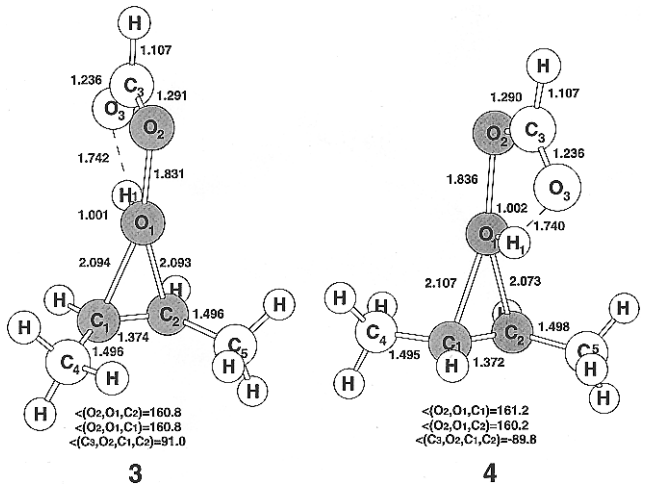

Figure 3. Selected geometrical parameters of the transition structures for the epoxidation of *cis*- and *trans*-2-butenes (**3** and **4**, respectively) with peroxyformic acid calculated at the B3LYP/6-31G* level.

transition structure **2d** with an "endo" or syn orientation of the HOOCHO fragment relative to the methyl group (Figure 2) is 0.4 kcal/mol higher in energy at the B3LYP/6-31G* level. Both approaches lead to first-order saddle points at this level. The barrier for the propene epoxidation is lower than that for ethylene (Table 3) in agreement with the experiment.[32]

In summary, in all the cases discussed above, the nature of transition structures calculated using the B3LYP functional agrees well with the results of higher correlated and more CPU intensive methods such as QCISD, QCISD(T), and CCSD. However, an applicability of the B3LYP calculations for each reaction type should be examined explicitly.[33] Although the B3LYP barriers are apparently underestimated, this method is obviously superior to the MP2 level in calculations of the transition state geometries of these alkene epoxidation reactions. The barriers for the ethylene and propene epoxidation reactions calculated at the QCISD(T)/6-31G* level using the B3LYP/6-31G* optimized geometries are very close to those computed at the much more computer-time demanding QCISD(T)/6-31G*//QCISD/6-31G* level (Table 3).

Epoxidation of *cis*- and *trans*-2-Butene by Peroxyformic Acid. The activation barrier of the *cis*-2-butene epoxidation reaction calculated at the B3LYP/6-31G* level is 10.1 kcal/mol (with the ZPE(B3LYP/6-31G*) correction). The C−O bond distances in the spiro ($\angle C_3O_2C_1C_2 = 91.0°$) transition structure (**3**) for the epoxidation of *cis*-2-butene are nearly identical (Figure 3). The first-order saddle point (**4**) for the epoxidation of the trans isomer is slightly higher in energy ($\Delta E^{\ddagger} = 10.6$ kcal/mol; Figure 3, Table 4). To find out whether diffuse functions are necessary to reflect effects of the oxygen lone pairs on the barrier height in the epoxidations of substituted alkenes, we also calculated these barriers for *cis*- and *trans*-2-

TABLE 4: Activation Barriers (in kcal/mol) for the Epoxidation of *cis*- and *trans*-2-Butene with Peroxyformic Acid Calculated at the B3LYP Computational Level[a]

computational level	*cis*-2-butene	*trans*-2-butene
B3LYP/6-31G*//B3LYP/6-31G*	10.0 (10.1)[b,c]	10.4 (10.6)
B3LYP/6-31+G*//B3LYP/6-31+G*	10.1 (10.1)	10.8 (10.9)

[a] The barrier heights are relative to the reactants. [b] The barriers with the ZPE(B3LYP) corrections (scaled with 0.98) are given in parentheses. [c] The B3LYP/6-31G* barrier for the transition structure with "endo" orientation of the HOOCO fragment is 10.7 kcal/mol (10.8 kcal/mol with the ZPE correction).

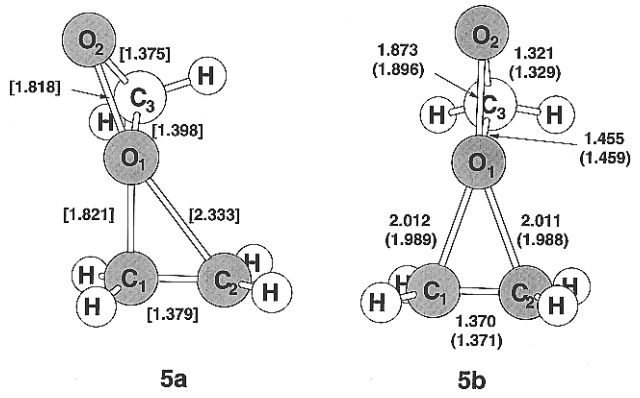

Figure 4. Selected geometrical parameters of the transition structures for the epoxidation of ethylene with dioxirane calculated at the MP2/6-31G* level (**5a**) as well as at the B3LYP/6-31G* (**5b**), MP2/6-31G* (**5b**), and QCISD/6-31G* (**5b**) levels of theory. The geometrical parameters of structure **5b** calculated at the QCISD/6-31G* and MP2/6-31G* levels are given in parentheses and in square brackets, respectively.

butenes using the more flexible 6-31+G* basis set, but found little difference (Table 4). As for the ethylene epoxidation reactions (Table 2), the B3LYP/6-31G* and B3LYP/6-31+G* barriers are also close to each other. In general, the rate for nonconjugated alkenes increases with the number of alkyl substituents.[32] Our data (B3LYP) suggest that each additional methyl group reduces the activation barrier by ≈2 kcal/mol reflecting a consistent lowering of the $\Delta E^{\neq}$ as the number of alkyl substituents increases. Thus, the predicted barrier of 10.1 kcal/mol for *cis*-2-butene ($\Delta H_{298}^{\ddagger} = 10.0$ kcal/mol, $\Delta S_{298}^{\ddagger} = -34$ cal/K mol) is in good agreement with that reported for the Z-disubstituted alkene cyclohexene ($\Delta H^{\ddagger} = 10.42$ kcal/mol, $\Delta S^{\ddagger} = -32.9$ cal/K mol).[8a]

Epoxidation of Ethylene by Dioxirane and Dimethyldioxirane. Dimethyldioxirane and several related peroxy species have been found recently to be powerful oxygen atom transfer reagents of unusual synthetic utility.[34] The MP2/6-31G* calculations lead to unsymmetrical transition structure **5a** (the distances between the spiro oxygen and the double-bond carbons are 1.821 and 2.333 Å, respectively; Figure 4)[9e] in a manner similar to that found in the MP2/6-31G* calculations of the ethylene epoxidation reaction. A structure constrained to be symmetrical (Figure 4) is 3.0 kcal/mol higher in energy than unsymmetrical transition structure **5a** at the MP2/6-31G* level.[9e] We therefore felt it is essential to examine the accuracy of the MP2 transition structure and provide a comparison with both DFT and QCISD methods. Unsymmetrical transition structure **5a** was used as starting point in the B3LYP/6-31G* calculations which resulted in symmetrical transition structure **5b** (C_s symmetry; the distance between the spiro oxygen and the double-bond carbons is 2.011 Å; Figure 4). As noted above for QCISD calculations of the transition structure for the epoxidation of ethylene by peroxyformic acid, the QCISD/6-31G* geometry optimization also leads to symmetrical transition

TABLE 5: Activation Barriers (in kcal/mol) for the Epoxidation of Ethylene with Dioxirane and Dimethyldioxirane Calculated at Various Computational Levels[a]

computational level	dioxirane	dimethyl-dioxirane
Unsymmetrical Transition Structures[b]		
MP2/6-31G*//MP2/6-31G*	13.4	10.8
MP4SDTQ/6-31G*//MP2/6-31G*	13.7	2.8
QCISD(T)/6-31G*//MP2/6-31G*	16.7	20.4
Symmetrical Transition Structures[c]		
QCISD(full)/6-31G*//QCISD(full)/6-31G*	22.6	25.7
QCISD(T)/6-31G*//B3LYP/6-31G*	16.4	19.3
B3LYP/6-31G*//B3LYP/6-31G*	12.9	17.9
QCISD(T)/6-31G*//QCISD(full)/6-31G*	16.6	19.4

[a] The barrier heights are relative to the isolated reactants. [b] **5a** and **6a** are the unsymmetrical transition structures for dioxirane and dimethyldioxirane, respectively. [c] **5b** and **6b** are the symmetrical transition structures for dioxirane and dimethyldioxirane, respectively.

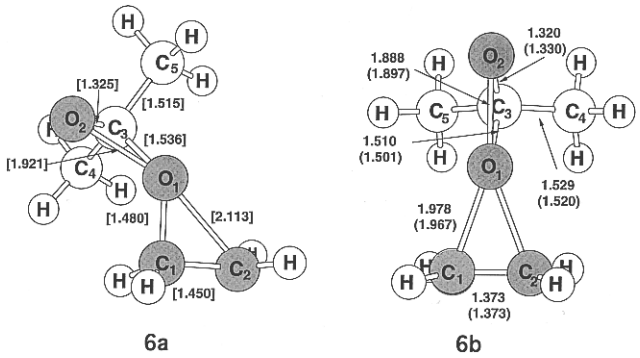

Figure 5. Selected geometrical parameters of the transition structures for the epoxidation of ethylene with dimethyldioxirane calculated at the MP2/6-31G* level (**6a**) as well as at the B3LYP/6-31G* (**6b**), MP2/6-31G* (**6b**), and QCISD/6-31G* (**6b**) levels of theory. The geometrical parameters of structure **6b** calculated at the QCISD/6-31G* and MP2/6-31G* levels are given in parentheses and in square brackets, respectively.

structure **5b** of C_s symmetry (Figure 4). While the RHF solution for symmetrical transition structure **5b** optimized at the B3LYP/6-31G* level exhibits an RHF → UHF instability (the negative eigenvalue of the stability matrix is −0.0419 hartrees), the B3LYP solution is triplet stable reflecting the effect of electron correlation treatment.

The activation barrier for the epoxidation of ethylene with dioxirane is lower at the B3LYP/6-31G* level (12.9 kcal/mol) when compared with the barriers computed at other levels of theory (Table 5). This barrier value is very close to the MP4SDTQ/6-31G*//MP2/6-31G* barrier of 13.7 kcal/mol despite considerable differences in the transition structure geometries. These data suggest that the parent dioxirane is a slightly more reactive oxygen donor toward ethylene than the peroxyformic acid. The barrier for dimethyldioxirane, however, increases significantly (Table 5), possibly reflecting the smaller energy gap between the ground and first excited state for dioxirane (11.6 kcal/mol)[35] compared with that for dimethyldioxirane (19.1 kcal/mol).[35]

Both the QCISD(full)/6-31G* and B3LYP/6-31G* calculations lead to a symmetrical spiro transition structure for the epoxidation of ethylene by dimethyldioxirane (Figure 5) with activation barriers of 25.7 and 17.9 kcal/mol, respectively. The triples contributions lower the QCISD barrier as noted above for peracid oxidation. It is notable that the transition structure geometries found at the QCISD(full)/6-31G* and B3LYP/6-31G* levels are also quite close to each other. Both symmetrical (resulting from a symmetry-constrained optimization) and

unsymmetrical structures were located during the search for a transition structure at the MP2/6-31G* level. The former has a 8.5 kcal/mol higher energy than the latter which we found to be a first-order saddle point at this level. The calculated MP2/6-31G* barrier height is 10.8 kcal/mol for the unsymmetrical first-order saddle point.[9e] Notably the MP4SDTQ/6-31G*//MP2/6-31G* calculations result in lowering the barrier for this highly skewed transition structure to just 2.8 kcal/mol possibly reflecting the instability of the wave function. In this instance both the barrier and the transition structure geometry differ considerably from those calculated at the QCISD(full)/6-31G* and B3LYP/6-31G* levels. Hence, the MP2/6-31G* geometry optimization is biased in favor of an unsymmetrical transition structure, whereas the B3LYP calculations predict a symmetrical transition structure like that found at higher correlated levels.[33] The barrier for the epoxidation of ethylene by dimethyldioxirane calculated at the QCISD(T)/6-31G*//B3LYP/6-31G* level (19.3 kcal/mol) is 6.4 kcal/mol lower than the QCISD/6-31G*//QCISD/6-31G* barrier (Table 5). However, as seen from the data for the ethylene epoxidation with peroxyformic acid, the triples contributions lead to a significant lowering (6.3 kcal/mol) of the barrier when compared with the QCISD value (Table 2), suggesting quite good agreement.

An Assessment of the B3LYP Calculated Barriers for the Epoxidation of Alkenes. Finally, we can make a general remark concerning the B3LYP calculated barrier heights. For all the epoxidation reactions, the barriers calculated using B3LYP are underestimated when compared with the QCISD and CCSD(T) results. A solution of this problem may be calculations of the barriers at the QCISD(T) level using the geometries optimized at the B3LYP level as discussed above. Another solution would be a temptation to increase the calculated barrier heights by increasing the contribution of the exchange terms in the B3LYP functional.[36] We feel, however, this would not make much sense because an adjustment of the calculated B3LYP barriers, for example, for S_N2 reactions[7s] could require a mixture of exchange terms which can be different for every reaction.[36b] The "half and half" functionals (e.g. BH&HLYP)[21] were reported to give the activation barriers for some simple radical reactions,[7e] proton transfer reactions,[37a] and amino acid decarboxylations[37b] that are not considerably underestimated when compared with the available experimental data or higher level computational results. While the B3LYP functional demonstrates a good performance in calculations of various properties of structures which are minima on the potential energy surface,[5] it is not clear, however, for now whether the use of a "half-and-half" or similar type functional is well-balanced for calculations of both reactants and transition structures of various reactions.[38]

To examine this question we have carried out calculations on the epoxidation of ethylene with peroxyformic acid using the BH&HLYP functional. The calculations have led to a symmetrical transition structure (Table 1) similar to that found at the B3LYP level. The main difference is that the transition structure geometry calculated using the BH&HLYP functional is tighter than that computed at CASSCF, QCISD, CCSD, and B3LYP levels (with shorter O_1C_1 and O_1O_2 bond distances, Table 1). The BH&HLYP/6-31G* calculated barrier (26.9 kcal/mol) (Table 2) is almost twice as high as the B3LYP barrier (14.1 kcal/mol). However, the BH&HLYP barrier is overestimated by up to 8 kcal/mol when compared with the barriers calculated at the QCSID(T) (18.8 kcal/mol), BD(T) (19.9 kcal/mol), and CCSD(T) (19.4 kcal/mol) levels of theory (Table 2). For the epoxidation of propene, the BH&HLYP/6-31G* calculations give a barrier of 24.5 kcal/mol (Table 3) that is close to the QCISD/6-31G* barrier of 22.3 kcal/mol, but considerably higher than that when the triples are included and the barrier is reduced to 16.0 kcal/mol. The O_1-C_1, O_1-C_2, and O_1-O_3 distances in the transition structure **2c** calculated using BH&HLYP are shorter than those found at the B3LYP and QCISD levels (Figure 2). Apparently, this reflects an overestimation of the bonding in the transition structure **2c** calculated at the BH&HLYP level. Similar to the computational results on the ethylene epoxidation (Table 2), the B3LYP6-31G* calculated barrier for the propene epoxidation (12.0 kcal/mol) is closer to the QCISD(T) value than the barrier height computed at the BH&HLYP level (Table 3). Density functional theory is currently the object of a great number of theoretical studies, and we can expect the development of better functionals in the forthcoming years.

4. Conclusions

Our study on the performance of the B3LYP DFT calculations on the epoxidation reactions for ethylene, propene, isobutene, and *cis*- and *trans*-2-butene with peroxyformic acid and for ethylene with dioxirane and dimethyldioxirane leads to the following conclusions:

(1) In contrast to the results of the MP2 calculations, the nature of the transition structures in the alkene epoxidation reactions calculated at the B3LYP level agree well with those computed using higher correlated methods such as QCI and CC. Therefore, while the MP2 calculations are biased in favor of unsymmetrical transition structures, the B3LYP method is capable of providing the correct transition structure geometry for simple unconjugated alkenes if the B3LYP solution is stable.

(2) The transition structures for the epoxidation of ethylene and propene with peroxyformic acid and of ethylene with dioxirane and dimethyldioxirane calculated at the B3LYP level as well as at the QCISD and CCSD levels are symmetrical with a spiro orientation of the electrophilic oxygen, whereas the MP2 calculations favor unsymmetrical transition structures. The geometries of the transition structures calculated using the B3LYP functional are close to those found at QCISD, CCSD, CCSD(T) levels as well as those found at the CASSCF(10,9) and CASSCF(10,10) levels for the transition structure of the epoxidation of ethylene.

(3) The activation barriers for the epoxidation reactions calculated at the B3LYP/6-31G* and B3LYP/6-31+G* levels are systematically lower (up to 5−6 kcal/mol) than the barrier heights calculated at such higher correlated levels as the QCISD(T)/6-31G*//QCISD/6-31G*, CCSD(T)/6-31G*//CCSD/6-31G*, and BD(T)/6-31G*//QCISD/6-31G*, although the transition structure geometries calculated at these levels of theory are in good agreement. In contrast, the BH&HLYP6-31G* barrier for the epoxidation of ethylene and propene with peroxyformic acid is overestimated by up to 8 kcal/mol when compared with the barriers calculated at the QCISD(T), BD(T), and CCSD(T) levels of theory. The activation barriers calculated at the QCISD(T)/6-31G*//B3LYP/6-31G* level appear to be close enough to those computed at the QCISD(T)/6-31G*//QCISD/6-31G* level to adopt this protocol for relatively large systems.

Acknowledgment. This work has been supported by the National Science Foundation (CHE-9531242) and a NATO Collaborative Research grant (900707). We are thankful to the Pittsburgh Supercomputing Center, National Center for Supercomputing Applications (Urbana, Illinois), CRAY Research, and the Ford Motor Co. for generous amounts of computer time. C.M.E. gratefully acknowledges a fellowship from the Xunta

de Galicia (Galicia, Spain) which has made his stay at the University of Delaware possible.

References and Notes

(1) (a) University of Delaware. E-mail: rbach@udel.edu. WWW http://udel.edu/~rbach. (b) Pittsburgh Supercomputing Center, Carnegie Mellon University. (c) Wayne State University. (d) Yale University.

(2) (a) Labanowski, J. K., Andzelm, J. W., Eds.; *Density Functional Methods in Chemistry*; Springer: New York, 1991. (b) Ellis, D. E., Ed.; *Density Functional Theory of Molecules, Clusters, and Solids*; Kluwer: Dodrecht, 1995. (c) Ziegler, T. *Chem. Rev.* **1991**, *91*, 651. (d) Ziegler, T.; Gutsev, G. I. *J. Comput. Chem.* **1992**, *13*, 70. (e) Li, J.; Schreckenbach, G.; Ziegler, T. *J. Phys. Chem.* **1994**, *98*, 4838. (f) Gutsev, G. I. *J. Chem. Phys.* **1993**, *98*, 7072. (g) Ricca, A.; Bauschlicher, C. W. *J. Phys. Chem.* **1994**, *98*, 12899. (h) Bauschlicher, C. W.; Maitre, P. *J. Phys. Chem.* **1995**, *99*, 3444. (i) Maitre, P.; Bauschlicher, C. W. *J. Phys. Chem.* **1995**, *99*, 6836. (j) Holthausen, M. C.; Heinemann, C.; Cornehl, H.; Koch, W.; Schwarz, H. *J. Chem. Phys.* **1995**, *102*, 4931. (k) Holhausen, M. C.; Mohr, M.; Koch, W. *Chem. Phys. Lett.* **1995**, *240*, 245. (l) Stanton, R. V.; Merz, K. M. *J. Chem. Phys.* **1994**, *100*, 434. (m) Jursic, B. S. *Chem. Phys. Lett.* **1996**, *256*, 603. (n) Kohn, W.; Becke, A. D.; Parr, R. G. *J. Phys. Chem.* **1996**, *100*, 12974. (o) Jursic, B. S. *J. Comput. Chem.* **1996**, *17*, 835. (p) Merrill, G. P.; Kass, S. R. *J. Phys. Chem.* **1996**, *100*, 17465.

(3) (a) Becke, A. D. *Phys. Rev. A* **1988**, *37*, 785. (b) Lee, C.; Yang, W.; Parr, R. G. *Phys. Rev.* **1988**, *B41*, 785.

(4) (a) Becke, A. D. *J. Chem. Phys.* **1993**, *98*, 5648. (b) Stevens, P. J.; Devlin, F. J.; Chablowski, C. F.; Frisch, M. J. *J. Phys. Chem.* **1994**, *98*, 11623.

(5) (a) Schleyer, P. v. R.; Jiao, H.; Glukhovtsev, M. N.; Chandrasekhar, J.; Kraka, E. *J. Am. Chem. Soc.* **1994**, *116*, 10129. (b) Bauschlicher, C. W.; Partridge, H. *Chem. Phys. Lett.* **1995**, *240*, 533. (c) Bauschlicher, C. W.; Partridge, H. *J. Chem. Phys.* **1995**, *103*, 1788. (d) Hertwig, R. H.; Koch, W. *J. Comput. Chem.* **1995**, *16*, 576. (e) Mebel, A. M.; Morokuma, K.; Lin, M. C. *J. Chem. Phys.* **1995**, *103*, 7414. (f) Glukhovtsev, M. N.; Pross, A.; Nicolaides, A.; Radom, L. *J. Chem. Soc., Chem. Commun.* **1995**, 2347. (g) Hay, P. J. *J. Phys. Chem.* **1996**, *100*, 5. (h) Stčkigt, D. *Chem. Phys. Lett.* **1996**, *250*, 387. (i) De Proft, F.; Martin, J. M. L.; Geerlings, P. *Chem. Phys. Lett.* **1996**, *250*, 393. (j) Tozer, D. J. *J. Chem. Phys.* **1996**, *104*, 4166. (k) Kneisler, J. R.; Allinger, N. L. *J. Comput. Chem.* **1996**, *17*, 757. (l) Bytheway, I.; Bacskay, G. B.; Hush, N. S. *J. Phys. Chem.* **1996**, *100*, 6023. (m) Glukhovtsev, M. N.; Bach, R. D.; Nagel, C. J. *J. Phys. Chem.* **1997**, *101*, 316.

(6) (a) Smith, B. J.; Radom, L. *Chem. Phys. Lett.* **1994**, *231*, 345. (b) Smith, B. J.; Radom, L. *Chem. Phys. Lett.* **1995**, *245*, 123.

(7) (a) Glukhovtsev, M. N.; Bach, R. D.; Pross, A.; Radom, L. *Chem. Phys. Lett.* **1996**, *260*, 558. (b) Torrent, M.; Duran, M.; Solà, M. *J. Mol. Struct. (THEOCHEM)* **1996**, *362*, 163. (c) Jursic, B. S. *J. Chem. Phys.* **1996**, *104*, 4151. (d) Durant, J. L. *Chem. Phys. Lett.* **1996**, *256*, 595. (e) Hrusák, J.; Friedrichs, H.; Schwarz, H.; Razafinjanahary, H.; Chermette, H. *J. Phys. Chem.* **1996**, *100*, 100. (f) Goldstein, E.; Beno, B.; Houk, K. N. *J. Am. Chem. Soc.* **1996**, *118*, 6036. (g) Glukhovtsev, M. N.; Bach, R. D.; Laiter, S. *J. Org. Chem.* **1997**, *62*, 4036.

(8) (a) Hoveyda, A. H.; Evans, D. A.; Fu, G. C. *Chem. Rev.* **1993**, *93*, 1307. (b) Plesnicar, B. In *The Chemistry of Peroxides*; Patai, S., Ed.; Wiley: New York, 1983; p 521. (c) *Ibid*. Cremer, D., 1983; p 1. (d) *Ibid*. Swern, D. **1971**; Vol. 2, p 355. (e) Finn. M. G.; Sharpless, K. B. *Asymmetric Synthesis* **1986**, *5*, 247. (f) Berti, G. *Topics in Stereochemistry*, Eliel, E. L., Allinger, N. L., Eds.; Wiley-Interscience: New York, 1973, Vol. 7, p 93.

(9) (a) Bach, R. D.; Willis, C. L.; Domagals, J. M. In *Applications of MO theory in Organic Chemistry*; Csizmadia, I. C., Ed.; Elsevier: Amsterdam, 1977; Vol. 2, p 221. (b) Bach, R. D.; Andrés, J. L.; Davis, F. *J. Org. Chem.* **1992**, *57*, 613. (c) Bach, R. D.; Owensby, A.; González, C.; Schlegel, H. B. *J. Am. Chem. Soc.* **1991**, *113*, 2338. (d) Bach, R. D.; Su, M.-D.; Schlegel, H. B. *J. Am. Chem. Soc.* **1994**, *116*, 5379. (e) Bach, R. D.; Andrés, J. L.; Owensby, A.; Schlegel, H. B. *J. Am. Chem. Soc.* **1992**, *114*, 7207. (f) Bach, R. D.; Winter, J. E.; McDouall, J. J. W. *J. Am. Chem. Soc.* **1995**, *117*, 8586. (g) Bach, R. D.; Canepa, C.; Winter, J. E.; Blanchette, P. E. *J. Org. Chem.*, in press.

(10) (a) Interestingly, a thorough high-level (G2) study of O−O bond dissociation energies established the MP2 level to be adequate for the energetics of most reactions involving O−O bond scission.[10b] (b) Bach, R. D.; Ayala, P. Y.; Schlegel, H. B. *J. Am. Chem. Soc.* **1996**, *118*, 12758.

(11) Some results of DFT calculations of molecular systems for which nondynamical correlation is important appear to be encouraging. For example, the energy difference between the C_{2v} and D_{3h} structures of ozone was calculated to be 29.2 kcal/mol at the B3LYP/TZ2Pf level,[5j] which agrees well with the CCSD(T)/[5s4p3d2f] value of 29.1 kcal/mol.[11b] The bond length in the O_3 C_{2v} structure calculated at the B3LYP level (1.256 Å)[5j] is, however, shorter than the CCSD(T) and experimental values (1.273 and 1.272 Å, respectively). (b) Lee, T. J. *Chem. Phys. Lett.* **1990**, *169*, 529.

(12) Bartlett, P. D. *Rec. Chem. Progr.* **1950**, *11*, 47.

(13) Hehre, W. J.; Radom, L.; Schleyer, P. v. R.; Pople, J. A. *Ab Initio Molecular Orbital Theory*; Wiley: New York, 1986.

(14) Frisch, M. J.; Trucks, G. W.; Schlegel, H. B.; Gill, P. M. W.; Johnson, B. G.; Robb, M. A.; Cheeseman, J. R.; Keith, T. A.; Peterson, G. A.; Montgomery, J. A.; Raghavachari, K.; Al-laham, M. A.; Zakrzewski, V. G.; Ortiz, J. V.; Foresman, J. B.; Cioslowski, J.; Stefanov, B. B.; Nanayakkara, A.; Challacombe, M.; Peng, C. Y.; Ayala, P. Y.; Wong, M. W.; Replogle, E. S.; Gomperts, R.; Andres, J. L.; Martin, R. L.; Fox, D. J.; Binkley, J. S.; DeFrees, D. J.; Baker, J.; Stewart, J. J. P.; Head-Gordon, M.; Gonzalez, C.; Pople, J. A. GAUSSIAN-94; Gaussian Inc.: Pittsburgh, PA, 1995.

(15) (a) Schlegel, H. B. *J. Comput. Chem.* **1982**, *3*, 214. (b) Schlegel, H. B. *Adv. Chem. Phys.* **1987**, *67*, 249. (c) Schlegel, H. B. In *Modern Electronic Structure Theory*; Yarkony, D. R., Ed.; World *Scientific*: Singapore, 1995; p 459.

(16) Pople, J. A.; Head-Gordon, M.; Raghavachari, K. *J. Chem. Phys.* **1987**, *87*, 5968.

(17) (a) Raghavachari, K.; Trucks, G. W.; Pople, J. A.; Head-Gordon, M. *Chem. Phys. Lett.* **1989**, *157*, 479. (b) Bartlett, R. J. *Ann. Rev. Phys. Chem.* **1981**, *32*, 359.

(18) Handy, N. C.; Pople, J. A.; Head-Gordon, M.; Raghavachari, K.; Trucks, G. W. *Chem. Phys. Lett.* **1989**, *164*, 185.

(19) Roos, B. O. *Adv. Chem. Phys.* **1987**, *67*, 399.

(20) Using ACES II (Advanced Concepts in Electronic Stucture Program System): Barlett, R. J.; Purvis, G. D., III; Fitzgerlad, G. B.; Harrison, R. J.; Rittby, M.; Sosa, C.; Lee, Y. S.; Trucks, G. W.; Cole, S. J.; Salter, E. A.; Pal, S.; Watts, J.; Laidg, W. D.; Magers, D. H.; Stanton, J. F.; Bernholdt, D.

(21) The implementation of the BH&HLYP functional in Gaussian-94 (Rev. D. and higher) is as follows: $E_{xc}^{BH\&HLYP} = 0.5E_x^{LSDA} + 0.5E_x^{HF} + 0.5\Delta E^{B88} + E_c^{LYP} + E_c^{VWN}$. Note that this formulation slightly differs from that proposed by Becke.[22]

(22) Becke, A. D. *J. Chem. Phys.* **1993**, *98*, 1372.

(23) (a) Lynch, B. M.; Pausacker, K. H. *J. Chem. Soc.* **1955**, 1525. (b) Schwartz, N. N.; Blumbergs, J. H. *J. Org. Chem.* **1964**, *29*, 1976. (c) Vilka, M. *Bull. Soc. Chim. Fr.* **1959**, 1401. (d) Renolen, P.; Ugelstad, J. *J. Chim. Phys.* **1960**, *57*, 634. (e) House, H. O.; Ro, R. S. *J. Am. Chem. Soc.* **1958**, *80*, 2428. (f) Ogata, Y.; Tabushi, I. *J. Am. Chem. Soc.* **1961**, *83*, 3440, 3444. (g) Curci, R.; DiPrete, R. A.; Edwards, J. O.; Modena, G. *J. Org. Chem.* **1970**, *35*, 740.

(24) Yamabe recently described a transition structure for the epoxidation of ethylene at the MP2/6-31G* level that exhibited an unsymmetrical approach of the electrophilic oxygen to the carbon−carbon double bond.[25] He also located an intermediate (B)[25] and a second transition structure on the MP2 surface. However, we have found that this intermediate does not exist on the QCISD/6-31G* energy surface. Furthermore, we had reported[9f] that oxygen atom transfer to ethylene proceeds in a nearly ideal spiro fashion at the QCISD, CCSD, and CCSD(T)/6-31G* levels of theory. An unsymmetrical transition structure for the ethylene epoxidation has not been found at these levels of theory that lead to symmetrical transition structure **1b**.[9f]

(25) Yamabe, S.; Kondou, C.; Minato, T. *J. Org. Chem.* **1996**, *61*, 616.

(26) The negative eigenvalue of the stability matrix[26a,b] is −0.0334 hartrees (RHF/6-31G*). For the Hartree−Fock instabilities, see, for example: (a) Seeger, R. R.; Pople, J. A. *J. Chem. Phys.* **1976**, *65*, 265. (b) Chambaud, G.; Levy, B.; Millie, P. *Theor. Chim. Acta* **1978**, *48*, 103. (c) Glukhovtsev, M. N.; Mestechkin, M. M.; Minkin, V. I.; Simkin, B. Ya. *Zh. Strukt. Khim. (USSR)* **1982**, *23*, 14. (d) Glukhovtsev, M. N.; Simkin, B. Ya.; Yudilevich, I. A. *Theor. Eksper. Khim. (USSR)* **1982**, *18*, 726. (e) Schlegel, H. B.; McDouall, J. J. W. In *Computational Advances in Organic Chemistry: Molecular Structure and Reactivity*; Ögretir, C., Csizmadia, I. G., Ed.; Kluwer: Dordrecht, 1991; p 167. (f) Chen, W.; Schlegel, H. B. *J. Chem. Phys.* **1994**, *101*, 5957.

(27) Hamilton, T. P.; Pulay, P. *J. Chem. Phys.* **1988**, *88*, 4926.

(28) The CASSCF(4,4)/3-21G calculations also lead to an unsymmetrical transition structure.[25]

(29) McLean, A. D.; Lengsfield, B. H., III; Pacansky, J.; Ellinger, Y. *J. Chem. Phys.* **1985**, *83*, 3567.

(30) The number of electronic configurations included in the (14, 10), (10, 9), and (10, 10) calculations are 4, 950; 5, 292; and 19, 404 respectively. The coefficients of the reference configurations for these three calculations are 0.85, 0.92, and 0.91.

(31) Valov, P. I.; Blyumberg, E. A.; Filippova, T. V. *Kinetika i Kataliz* **1967** *8*, 760.

(32) The relative rates of expoxidation of ethylene, propene, styrene, isobutylene, and 2-butene with peracetic acid are 1, 22, 59, 484, and 489, respectively.[8a,b]

(33) (a) The RHF → UHF instability of the B3LYP solution for the transition structure is crucially important for a correct description of transition structures for alkene epoxidation reactions. If the B3LYP solution is triplet unstable as it is observed for the epoxidation of ethylene with peroxynitrous acid, HOONO,[33b,c] the B3LYP calculations tend to give rise to a less symmetrical transition structure, in contrast to the QCISD results that lead to a symmetrical transition structure. (b) Bach, R. D.; Glukhovtsev, M. N.; Canepa, C. *J. Am. Chem. Soc.*, submitted. (c) For a recent study of

the epoxidation of alkenes with peroxynitrous acid, see: Houk, K. N.; Condroski, K. R.; Pryor, W. A. *J. Am. Chem. Soc.* **1996**, *118*, 13002.

(34) Adam, W.; Haas, W.; Lohray, B. B. *J. Am. Chem. Soc.* **1991**, *113*, 6202 and relevant references therein.

(35) (a) The energy differences between the ground and first excited singlet states for dioxirane[9e] and dimethyldioxirane[35b] were calculated at the QCISD(T)/6-31G*//MP2/6-31G* level. (b) Bach, R. D.; Baboul, A. G.; Schlegel, H. B. Manuscript in preparation.

(36) (a) Becke, A. D. In *Modern Electronic Structure Theory*; Yarkony, D. R., Ed.; World Scientific: Singapore, 1995; p 1022. (b) Baker, J.; Andzelm, J.; Muir, M.; Taylor, P. *Chem. Phys. Lett.* **1995**, *237*, 53.

(37) (a) Zhang, Q.; Bell, R.; Truong, T. N. *J. Phys. Chem.* **1995**, *99*, 592. (b) Bach, R. D.; Canepo, C. *J. Am. Chem. Soc.*, submitted.

(38) We calculated overall barriers (i.e. barriers relative to the isolated reactants) for the $F^- + CH_3F$ and $Cl^- + CH_3Cl$ gas phase S_N2 reactions at the BH&HLYP/6-31+G* level. These reactions have been studied well, both experimentally and computationally (for example, see ref 39 and relevant references therein), and this allows us to evaluate the performance of the BH&HLYP functional. The BH&HLYP calculated overall barriers (without ZPE corections) are 2.8 (Cl) and −0.5 (F) kcal/mol. These values are close to the G2 values of 2.7 (Cl) and −1.9 (F) kcal/mol and to the experimental estimate of the barrier for the $Cl^- + CH_3Cl$ reaction (2.5 kcal/mol).[40] The overall barrier for the chloride exchange is underestimated at the B3LYP/6-31+G* level (−0.9 kcal/mol; without ZPE corrections), whereas the MP2/6-31+G* calculated barrier is 7.7 kcal/mol. However, the BH&HLYP calculations can give an incorrect type of stationary point on the potential energy surface. For example, the D_{6h} structure of hexazine (N_6) is calculated to be a minimum (the lowest frequency (e_{2u}) is 95 cm^{-1}) at the BH&HLYP/6-31G* level, in contrast to the MP2/6-31G* and B3LYP/6-31G* results[41] indicating that this structure corresponds to a second-order saddle point.

(39) (a) Glukhovtsev, M. N.; Pross, A.; Radom, L. *J. Am. Chem. Soc.* **1995**, *117*, 2024. (b) Glukhovtsev, M. N.; Pross, A.; Schlegel, H. B.; Radom, L.; Bach, R. D. *J. Am. Chem. Soc.* **1996**, *118*, 11258.

(40) Barlow, S. E.; Van Doren, J. M.; Bierbaum, V. M. *J. Am. Chem. Soc.* **1988**, *110*, 7240.

(41) (a) Glukhovtsev, M. N.; Schleyer, P. v. R. *Chem. Phys. Lett.* **1992**, *198*, 547. (b) Glukhovtsev, M. N.; Jiao, H.; Schleyer, P. v. R. *Inorg. Chem.* **1996**, *35*, 7124.